

Dynamical disorder of spin-induced Jahn-Teller orbitals with the insulator-metal transition in cobaltates

Despina Louca¹ and J. L. Sarrao²

¹University of Virginia, Department of Physics, Charlottesville, VA 22904.

²Los Alamos National Laboratory, Los Alamos, NM 87545.

(Dated: April 14, 2024)

Abstract

Using elastic and inelastic neutron scattering, we investigated the evolution of the local atomic structure and lattice dynamics of $\text{La}_{1-x}\text{Sr}_x\text{CoO}_3$ ($x = 0-0.5$) as it crosses over with x from an insulator to a ferromagnetic metal (FMM). Our pair density function analysis indicates that in the paramagnetic insulating (PMI) phase for all x , spin activation of Co^{3+} ions induces local static Jahn-Teller (JT) distortions. The size of the JT lattice increases almost linearly with x : However, in the FMM phase, static JT distortions are absent for $x \leq 30\%$. This coincides with narrowing of $\omega \approx 22$ and 24 meV modes in the phonon spectrum in which we argue is due to localized dynamical JT fluctuations. For $x > 30\%$, static JT distortions reappear along with broadening of the phonon modes because of weakened charge-lattice interactions.

PACS numbers: 61.12.-q, 71.70.-d, 71.30.+h

Jahn-Teller (JT) interactions in transition metal perovskites have often led to quite interesting physical phenomena through the interplay of orbital and spin degrees of freedom with the lattice [1]. Understanding the characteristics of JT instability can help elucidate the nature of insulator-metal transitions (IMT), magnetoresistance and even superconductivity in a variety of systems [2]. It appears that in pure systems such as LaCoO_3 [3], LaMnO_3 [4] and YTiO_3 [5], cooperative JT or orbital ordering effects can exist up to very high temperatures. LaCoO_3 is distinctly different from other perovskite crystals because orbital degeneracy is created by themally inducing a spin transition [6] subjecting the system to variable spin-lattice coupling depending on the configuration [7]. The ground state of Co^{3+} ions at the octahedral sites is the low spin configuration (LS), $S=0$ $t_{2g}^6 e_g^0$, and this can be themally excited to either a high-spin (HS) $t_{2g}^4 e_g^2$ ($S=2$) or an intermediate-spin (IS) $t_{2g}^5 e_g^1$ ($S=1$) configuration [8]. Previous experimental [7,9] and theoretical [10] works showed that below room temperature the IS state is more stable than the HS because activation to this state invokes stronger oxygen p to cobalt d hybridization. The IS is distinct from the other two because it is e_g JT active: partial e_g occupancy induces orbital degeneracy which is lifted by changing the local crystal symmetry resulting in JT modes. Although in an ideal cubic perovskite the crystal field energy is large [11], strong Co-O covalency reduces the splitting between the t_{2g} and e_g bands that enables the transition to IS. In addition, the LS-IS transition might instigate dynamic orbital ordering [3, 10]. However, it is still unclear whether or not ordering, either static or dynamic, occurs when charge carriers are introduced to drive the system through an IMT.

The addition of charge carriers establishes the FMM state by $x > 18\%$ in $\text{La}_{1-x}\text{Sr}_x\text{CoO}_3$ [12], but little is known on the evolution of the spin transitions or the dependence of JT ordering to carrier mobility. Experimental evidence suggests that the IS-JT state is stabilized with doping at least in the PM I phase [7,13,14]. In the FMM, it would be conceivable that charge dynamics interfere with orbital JT ordering giving rise to a new state. When charge mobility increases, the JT distortions can lose their long-range coherency. But they might also fluctuate dynamically possibly giving rise to dynamical orbital ordering. Such dynamical JT modes can manifest themselves as real-space modulations of orbital waves or orbitons as suggested by Saitoh et al. [15] for LaMnO_3 . At the same time, such modes can also couple to the lattice forming polarons [16] or JT-polarons [17] depending on the coupling strength. On the other hand, in the absence of any ordering, a disordered structure

state would emerge, creating an orbital liquid state in an analogous way to geometrically frustrated magnetic systems [18]. In this paper we report on how the local atomic structure and lattice dynamics change from the PM I to the FM M phases in doped $\text{La}_{1-x}\text{Sr}_x\text{CoO}_3$ in support of JT dynamical orbital disorder.

We investigated $\text{La}_{1-x}\text{Sr}_x\text{CoO}_3$ using time-of-flight pulsed neutron scattering. The time-averaged structure function, $S(Q, \omega = 0)$, and the dynamical, time-resolved $S(Q, \omega)$ are combined to provide information on the type of atomic distortions and how they fluctuate in time. Characteristic energies of the fluctuations are defined that help explain the crossover from static to dynamic lattice effects. Our measurements indicate that lattice dynamics change continuously through the IM T both as a function of temperature and carrier concentration. Below the percolation limit, $x \approx 0.3$, the phase transition results from a break from an orbitally ordered, inferred from the presence of static JT in the PM I, to a JT disordered state due to dynamical fluctuations coupled to the increase in charge mobility. While the short-range local atomic structure sensitively follows the disappearance of ordering of JT distortions close to the phase boundary, the dynamical structure function shows that low-energy cobalt phonon modes get narrower in energy with cooling. The fact that JT disorder can create a local phonon resonance, $\omega \approx 22$ meV, might be a manifestation of a phonon mediated charge transfer mechanism that plays an important role in the transition process of $\text{La}_{1-x}\text{Sr}_x\text{CoO}_3$. Above the percolation concentration, connectivity between FM clusters is established that allows easy charge propagation accompanied by the reappearance of static JT and smearing of the phonon modes. In this case the lattice and charge dynamics are decoupled.

The powder samples were prepared by standard solid-state reaction method starting from SrCO_3 , La_2O_3 and Co_3O_4 , fired at 1100 °C with a final firing at 1300 °C in air, and additional annealing in nitrogen at 900 °C to ensure stoichiometric oxygen content for the pure sample. The neutron data were collected at the Intense Pulsed Neutron Source (IPNS). Data for the local structure analysis were obtained at the Glass Liquid and Amorphous Diffractometer (GLAD). The total $S(Q)$, integrated over a finite energy window and corrected for instrumental background, absorption, incoherent, multiple, and inelastic scattering, was Fourier transformed to determine the pair density function (PDF). The PDF provides a real-space representation of atomic pair correlations. Details of this technique can be found in ref. [19, 20]. The inelastic measurements were performed at

the Low Resolution Medium Energy Chopper Spectrometer (LRMECS). The incoming energy was set at $E_i = 35$ meV. Corrections for background and detector efficiency, empty aluminum can with and without cadmium shielding and vanadium standard measurements were performed. The data were also corrected for the sample self-shielding as well as the $\frac{k_f}{k_i}$ phase space factor. The data represent the sum over all scattering angles multiplied by the Bose population factor.

The temperature dependence of the PDF corresponding to the local atomic structure for $x = 0.1$ is shown in Fig. 1(a) in the vicinity of the Co-O octahedra. The Co-O pair correlation appears 1.93 Å as the first peak in the PDF since it is the shortest distance in the crystal. In the PM I phase, this peak is split and a second peak appears as a shoulder to the right 2.10 Å corresponding to long Co-O bonds. The presence of the small second peak is attributed to static JT distortions, similarly observed in LaMnO_3 [20], a well known JT system. In response to this local symmetry breaking, oxygen p and cobalt d hybridization is stabilized by minimizing Coulomb repulsions. Consequently, the crystal structure is expected to deviate from cubic symmetry because the Co-O octahedra elongate in the direction of the occupied orbital [7]. Below the spin-glass transition however ($T_{SG} = 45$ K), the peak corresponding to the long bonds vanishes while the main Co-O peak becomes taller. In Fig. 1(b) the presence of the long (LB) and short (SB) bonds is marked over an expanded temperature range. They are simultaneously present at temperatures above the transition while below only one type of bond is observed. For higher concentrations, the local atomic structure also shows evidence for JT distortions in the PM I phase (Fig. 2a). In the FM M however, JT distortions are not observed below $x_c = 0.3$ (Fig. 2b).

While it is expected that the number of IS-JT sites will be thermally populated as in LaCoO_3 , how that number varies with x is not well understood. An estimate of the JT population can be determined from the integrated intensity of the first Co-O PDF peak using the expression of ref. [21]. In the simplest scenario, one could assume that the addition of charge creates LS-Co^{4+} ions with all spins in the t_{2g} . Its local structure is therefore equivalent to that for LS-Co^{3+} . Thus in the insulating state, since charges remain localized at Co^{4+} sites, the area under the Co-O peak should remain constant. The combined intensity for LS-Co^{3+} and LS-Co^{4+} ions should account for the total area under the peak. In an ideal octahedral environment, the Co-O bonds are all short without JT and the coordination should be 6 corresponding to 100% LS. But as seen from Fig. 2c, the total

LS population corresponding to the number of Co-O undistorted octahedra decreases from 100 % with doping as strong indication that activation to a different spin state must be occurring. Unless we assume the presence of a third configuration, that of IS-JT, the total intensity can never be accounted for. The estimated dependence of LS-Co⁴⁺, total LS (Co⁴⁺ + Co³⁺) and IS-Co³⁺ to the nominal charge concentration are shown in Fig. 2 (c) at room temperature (RT). The split of the Co-O bonds is confirmed by Fig. 2 (a) and 2 (d) at RT, which is additional evidence for the IS-JT. Why is the IS-Co³⁺ activation linear? One possibility is that localized charges on LS-Co⁴⁺ in the insulating phase stabilize the JT at neighboring sites creating IS-Co³⁺. The contributing factors to this are size effects and covalency [22]: LS-Co⁴⁺ is smaller and intermediate oxygens shift towards it while stabilizing e_g orbital occupancy on neighboring IS-Co³⁺. The covalency between Co³⁺ and Co⁴⁺ is optimized by the e_g orbital occupancy and allows hopping. Such a pair would be coupled ferromagnetically with hopping occurring via e_g forming a Zener polaron. Thus for every Co⁴⁺ there would be an IS-Co³⁺ giving rise to the linear dependence on x (Fig. 2c). On the other hand, if activation to IS-Co⁴⁺ were to be considered, this would imply LS-Co³⁺ but that would be energetically unfavorable for e_g hopping.

Below the phase boundary, static JT distortions disappear, and at 10 K, the local structure appears uniform with no distortions, and the long and short Co-O bonds are indistinguishable for x > 0.3 (Figs. 2b and 2d). But the transition to the metallic state is not straight forward because of lattice dynamics implications. Plots of the dynamic structure function, S(Q), summed over all momentum transfers, Q, for 0, .1, .3 and .4 are shown in Fig. 3. With Sr doping, the shape and relative intensity of distinct low energy modes observed in the range of 10 to 30 meV change. In the pure sample, we observed that the band at 22 meV is suppressed relative to the 24 meV peak. Increasing x to 0.1 (spin-glass), the two bands are equal in height but not well resolved. But by x = 0.3, their intensity is enhanced and they become narrow and better resolved signifying an unusual electron-lattice interaction. The functions were fit by two gaussians in the 18-28 meV range (solid lines). The intensity exhibits a dependence on the momentum transfer proportional to Q² suggesting that they are primarily phononic in nature. Also the magnitude is indicative of many phonons being affected at once. The S(Q) plots were compared to the isostructural LaAlO₃ (not shown), another perovskite with the same rhombohedral symmetry and similar tilting along the [111] plane [23] which showed evidence for the low energy modes (10

and 15 meV) but shifted by ~2 meV to higher energies because of mass differences of Co and Al. However, the higher modes (22 and 24 meV) were absent in the aluminate which would suggest that the octahedra are inactive in this system. The results on the cobaltates differ from the IR measurements of ref. [24] that concluded that the phonons do not change with Sr doping based upon information on zone-center modes alone. For $x = 0.4$, static JT distortions reappear as seen in Fig. 2b concomitant while the 22 and 24 meV modes smear out and can be fit by a single gaussian centered at ~23 meV.

The development of the phonon modes particularly at 22 meV might be due to the formation of new Co-O lattice vibrations with the IMT. The observed changes are not due to a change in symmetry as the structure remains rhombohedral ($R\bar{3}C$ symmetry [13, 23]) on average at all x . Even though Sr is lighter than La, the peaks are not shifting to higher energies suggesting that these modes are not dominated by the La/Sr density of states. This is also supported by the fact that identical measurements on $LaAlO_3$ showed no such band formation. The evolution of $S(\omega)$ with temperature through the IMT is shown in Fig. 4 for the $x=0.30$ with $T_C \approx 240$ K. These bands may signify strong charge-lattice coupling in the metallic state that is either suppressed or smeared out in the insulating phase. The width of the peaks gets narrower below the IMT suggesting phonon localization.

If a $LS-Co^{4+}$ ion and an $IS-Co^{3+}$ ion are next to each other, by moving an e_g electron from Co^{3+} ion to a Co^{4+} ion they swap configuration. Therefore they can form a resonant state by dynamically sharing an e_g electron. The shared e_g electron can couple the t_{2g} electrons of the two ions ferromagnetically through double exchange. As the hole doping is increased, such pairs will start to connect with each other, forming a larger conducting network, and the entire lattice will change into a ferromagnet. In this system, the crystal field splitting between the e_g state and the t_{2g} state is of the order of $\Delta = 2$ eV [11]. In the undoped state this is large enough to overcome the Hund's coupling and the difference in the Coulomb repulsion for placing 2 electrons on the t_{2g} and that for placing 1 electron each on the t_{2g} state and the e_g state, and thus to drive the system to the LS state. In the doped state, however, the sharing of the e_g electron described above creates a strong Co-O-Co bond and reduces the magnitude of Δ , producing soft Jahn-Teller modes that are low enough in energy to be strongly populated by thermal phonons. Such a soft phonon mode could be the vehicle that induces the IMT. At higher doping, beyond the site percolation limit of 0.31 for a cubic lattice [25], the local structure shows the reappearance of static JT

distortions even in the metallic state. This might be because the concentration of charges is so high that propagation occurs through well connected LS-C⁴⁺ sites without destroying the JT at LS-C³⁺ sites.

It is possible that the observed effects also describe frustration of a JT lattice. In dilute JT crystals with a magnetic transition, a spin-glass phase can sometimes exist [26]. This is brought about when the magnetic moment is randomly distributed in space but frozen in specific directions, in clusters, while correlation between clusters exists. Fluctuations of spins can induce frustration of the JT lattice sites that can destroy their cooperativeness and give rise to a spin-glass like state [27,28]. This also affects the effective long-range elastic interactions between JT sites that can fluctuate in sign and magnitude. Such JT-spin interactions are believed to be quite uncommon [27] although glassy behavior is widely observed in ferroelectrics and might be the case for $\text{La}_{1-x}\text{Sr}_x\text{CoO}_3$. For comparison we note that the energy scale of the dynamics invoked by such interactions are intermediate to those of the manganites and cuprates. In manganites it is understood that the JT distortions are frozen. On the other hand in the cuprates when distortions are static one obtains stripe structures but when they are dynamic, as in the superconducting state, they are averaged out. The cobaltate system's intermediate behavior makes it a prototypical example for probing the nature of the crossover regime. In conclusion, the local atom structure combined with the dynamic structure function provided evidence for a phonon mediated transition mechanism for the IMT in $\text{La}_{1-x}\text{Sr}_x\text{CoO}_3$.

The authors would like to acknowledge valuable discussions with J.B. Goodenough, D. I. Khomskii and T. Egami. They also thank E. Goren ychkin and R. Osborn for their help with the LRM ECS experiment and data analysis. Work at the University of Virginia is supported under U.S. Department of Energy, under contract DE-FG 02-01ER 45927, at the Los Alamos National Laboratory under contract W-7405-Eng-36 and at the IPNS under contract W-31-109-Eng-38.

- [1] J.B. Goodenough, Mater. Res. Bull. 6, 967 (1971).
- [2] I.B. Bersuker, Chem. Rev. 101, 1067 (2001).
- [3] Y. Tokura and N. Nagaosa, Science 288, 462 (2000).
- [4] T. Mizokawa and A. Fujimori, Phys. Rev. B 51, 12880 (1995).
- [5] C. Ulrich et al, Phys. Rev. Lett 89, 167202 (2002).
- [6] J.B. Goodenough, J. Phys. Chem. Solids 6, 287 (1958).

- [7] D. Louca et al., Phys. Rev. B 60, R10378 (1999).
- [8] P. M. Raccach and J. B. Goodenough, Phys. Rev. 155, 932 (1967).
- [9] S. Stölen et al., Phys. Rev. B 55, 14103 (1997); T. Saitoh et al., Phys. Rev. B 56, 1290 (1997); V. G. Bhide et al., Phys. Rev. B 12, 2832 (1975); M. Abbate et al., Phys. Rev. B 47, 16124 (1993); K. Asai et al., Phys. Rev. B 50, 3025 (1994); M. Itoh and I. Natori, J. Phys. Soc. Japan 64, 970 (1995); S. Yamaguchi, Y. Okimoto, and Y. Tokura, Phys. Rev. B 55, R8666 (1997).
- [10] M. A. Korotin et al., Phys. Rev. B 54, 5309 (1996).
- [11] A. R. West, Solid State Chemistry and its Applications (John Wiley & Sons Ltd., Chichester, 1984), p. 306.
- [12] G. H. Jonker and J. H. Van Santen, Physica (Amsterdam) 19, 120 (1953).
- [13] R. Caciuc et al., Phys. Rev. B 59, 1068 (1999).
- [14] J. Wang et al., Phys. Rev. B 66, 064406 (2002); S. Tsubouchi et al., *ibid* 66, 052418 (2002).
- [15] E. Saitoh et al., Nature 410, 180 (2001).
- [16] L. F. Feiner, A. M. Oles, J. Zaanen, Phys. Rev. Lett. 78, 2799 (1997).
- [17] D. Louca et al., Phys. Rev. B 56, R8475 (1997).
- [18] S. Ishihara, M. Yamataka, and N. Nagaosa, Phys. Rev. B 56, 686 (1997); M. V. Mostovoy and D. I. Khomskii, cond-mat/0201420 v1.
- [19] B. H. Toby and T. Egami, Acta Crystallogr. A 48, 336 (1992).
- [20] D. Louca and T. Egami, Phys. Rev. B 59, 6193 (1999).
- [21] The number of C-O pairs is obtained from $N_{C-O} = \frac{\int_{r_1}^{r_2} 4\pi b^2(r) r^2 dr}{2c_o b_o}$ where r_1 and r_2 include only the first peak, $b(r)$ is the PDF, b_{C-O} is the neutron scattering lengths for C and O, $\langle b \rangle$ is the average scattering length and c_o is the concentration of C atoms per unit cell.
- [22] T. Mizokawa et al., Phys. Rev. B 63, 024403 (2000).
- [23] H. D. Megaw and C. N. W. Darrington, Acta Crystallogr. A 31, 161 (1975).
- [24] S. Tajima et al., J. Phys. C: Solid State Phys. 20, 3469 (1987).
- [25] R. Zallen, The Physics of Amorphous Solids (John Wiley & Sons, Inc., New York, 1983) p. 170.
- [26] F. Mehran and K. W. H. Stevens, Phys. Rev. B 27, 2899 (1983).

[27] M. D. Kaplan and B. G. Vekhter, Cooperative Phenomena in Jahn-Teller Systems (Plenum, New York, 1995), p. 112.

[28] A. V. Babinskii et al., Pis'ma Zh. Eksp. Teor. Fiz 57, 289 (1993).

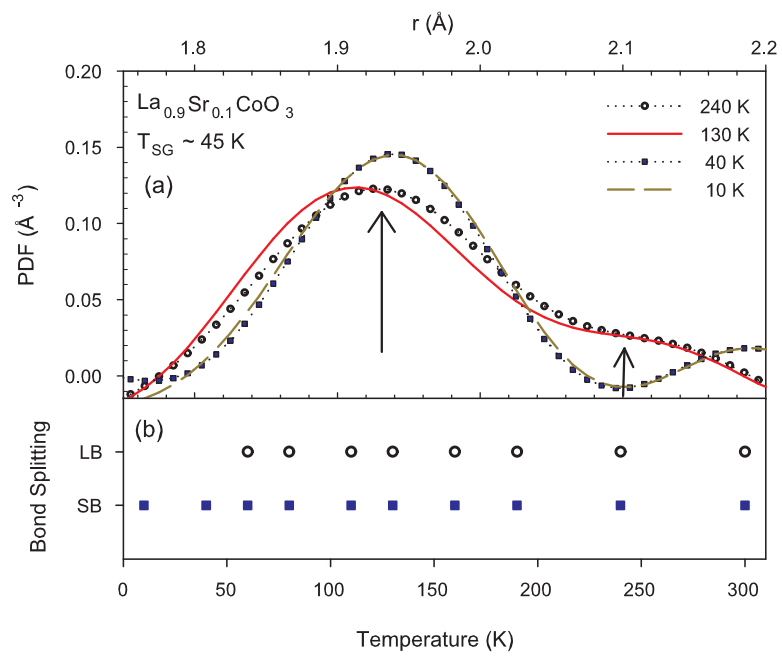
Figure captions:

Figure 1: (a) The PDF corresponding to the local atomic structure for $x = 0.1$ at representative temperatures is shown in the region of the Co-O peak. (b) Split of the Co-O peak to short (SB) and long (LB) bonds at all measured temperatures.

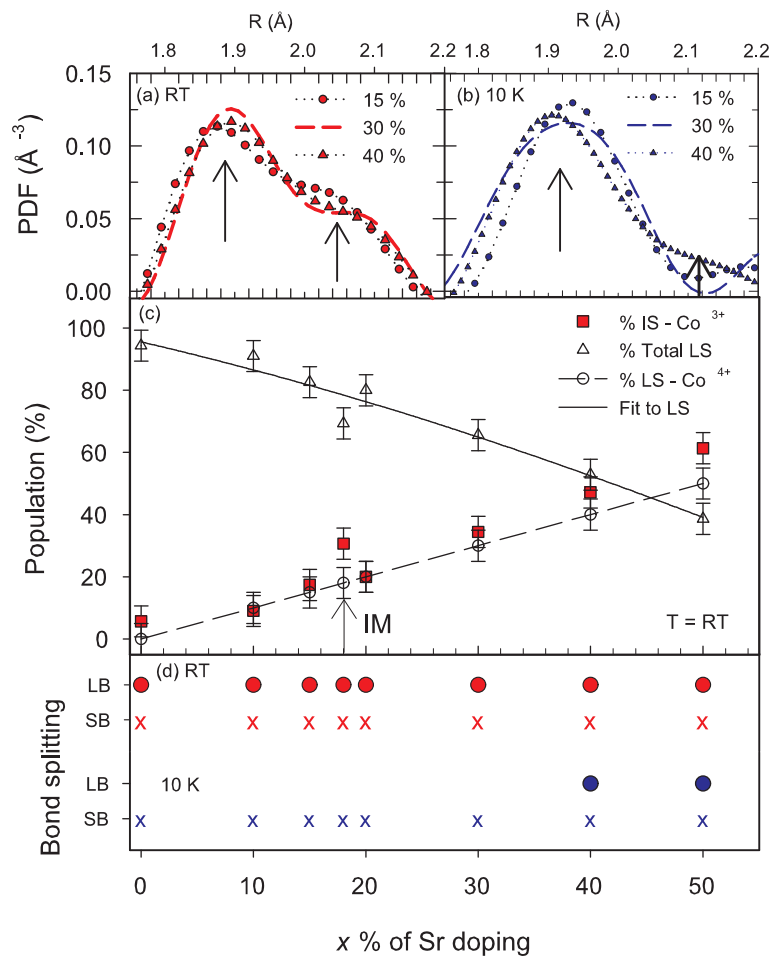
Figure 2: The Co-O PDF peak is shown for 3 compositions at (a) RT and (b) 10 K. (c) The percent population is estimated for LS-Co⁴⁺ assuming localized charges to single sites, total LS sites that combine LS-Co⁴⁺ and LS-Co³⁺, and IS-Co³⁺ ions in the PM I. Deviations from 100% are a strong indication for the presence of the third state, that of JT-Co³⁺. (d) The composition dependence of the long (LB) and short (SB) Co-O bonds plotted at RT and 10 K.

Figure 3: A plot of $S(\omega)$ determined for $x = 0, 0.1, 0.3$ and 0.4 at 10 K. Two gaussian functions (centered at 22 and 24 meV) are fit for 0, 0.1 and 0.3 and one for 0.4 (centered at 23 meV). The band formation around 22 meV is clearly separated by 0.3 and signifies an unusual electron-lattice interaction in the metallic state. In 0.4 the two bands merge to ones.

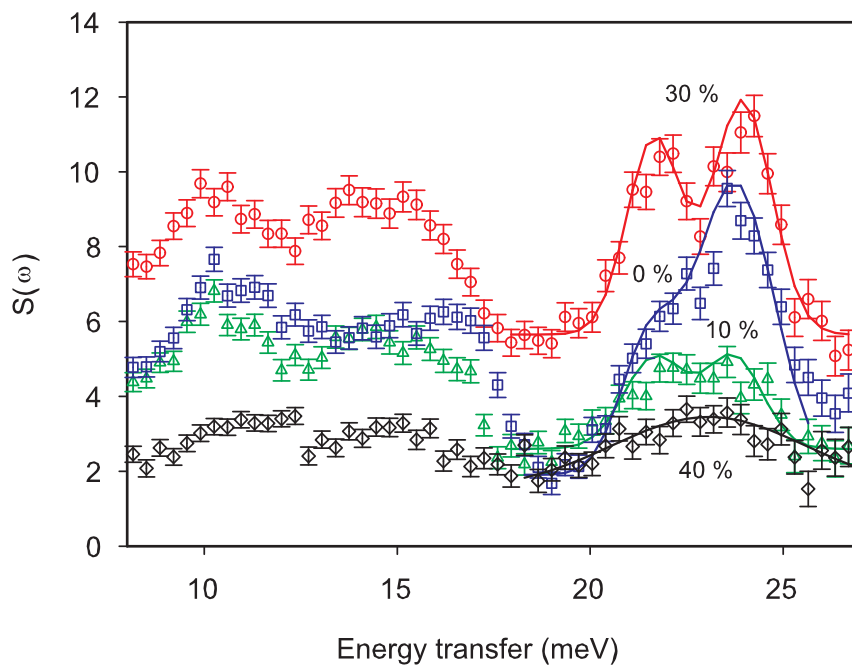
Figure 4: The temperature dependence of $S(\omega)$ expanded around 19-28 meV for 30% shows how the two modes become narrower through the IMT.

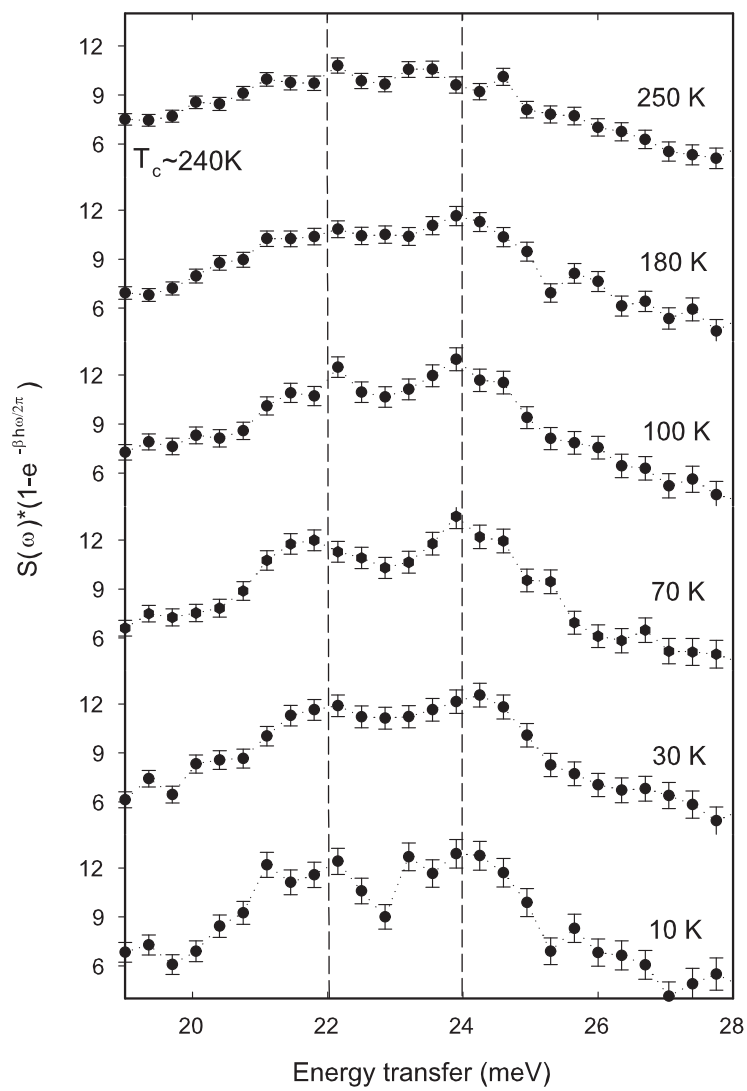


Louca et al., Fig. 1



Louca et al., Fig. 2





Louca et al., Fig. 4